Journal of Materials Chemistry C

PAPER

View Article Online
View Journal | View Issue

Cite this: J. Mater. Chem. C, 2014, 2, 4737

Synthesis and electroluminescence properties of highly efficient dual core chromophores with side groups for blue emission†

Hayoon Lee,‡[a] Beomjin Kim,‡[a] Seungho Kim,[a] Joonghan Kim,[a] Jaehyun Lee,[a] Hwangyu Shin,[a] Ji-Hoon Lee[b] and Jongwook Park*[a]

Received 13th January 2014
Accepted 22nd March 2014

DOI: 10.1039/c4tc00075g

www.rsc.org/MaterialsC

Highly efficient blue emitting materials consisting of dual core derivatives with phenyl and/or naphthyl side groups and asymmetric or symmetric structures were designed and synthesized. The asymmetric structures 1-naphthalen-1-yl-6-(10-phenyl-anthracen-9-yl)-pyrene (Ph-AP-Na) and 1-(10-naphthalen-1-yl-anthracen-9-yl)-6-phenyl-pyrene (Na-AP-Ph), and the symmetric structures 1-phenyl-6-(10-phenyl-anthracen-9-yl)-pyrene (Ph-AP-Ph) and 1-naphthalen-1-yl-6-(10-naphthalen-1-yl-anthracen-9-yl)-pyrene (Na-AP-Na) were synthesized. Of the synthesized compounds, Na-AP-Na was found to exhibit the highest EL device efficiency of 5.46 cd A^{-1}. Ph-AP-Na, Na-AP-Ph, Ph-AP-Ph, and Na-AP-Na exhibit EL maximum values of real blue color in the range 455 nm to 463 nm. The *y* values of their color coordinates are within the range 0.125 to 0.142, so these compounds exhibit good blue color coordinates for displays. The lifetime of the Na-AP-Na device was more than three times longer than that of the AP dual core (1-anthracen-9-yl-pyrene) device.

Introduction

Since the study of organic light-emitting diodes (OLEDs) began, OLEDs have received much attention because of their potential applications in full-color flat panel displays and next generation lighting.[1–6] In order to fabricate full color OLED displays, we need high performance red-light, green-light, and blue-light emitters with high electroluminescence (EL) efficiencies, good thermal properties, long device lifetimes, and pure color coordinates.[7–17] A red-light emitter with $CIE_{x,y}$ coordinates of (0.66, 0.34) and a long lifetime of more than 600 000 h (half lifetime@1000 cd m^{-2}) at 24 cd A^{-1} has recently been developed. A green-light emitter with $CIE_{x,y}$ coordinates of (0.34, 0.62) and a lifetime of 400 000 h (half lifetime@1000 cd m^{-2}) at 78 cd A^{-1} has also been achieved.[18] However, the best official results for a blue-light emitter with fluorescence materials are a short lifetime of only 10 000 h at 9.0 cd A^{-1} and $CIE_{x,y}$ coordinates of (0.14, 0.12).[19] The development of a blue emitter with high color purity, high efficiency, and a long lifetime has proved extremely challenging. It is difficult to produce highly efficient blue light emitters with long device lifetimes because, with a wide band gap, their electronic levels are likely to be mismatched with the highest occupied molecular orbital (HOMO) and lowest unoccupied molecular orbital (LUMO) levels of the other OLED layers such as the hole transporting layer (HTL) and the electron transporting layer (ETL). These differences between the electronic levels result in a mismatched carrier balance of electrons and holes, a low EL efficiency and a short lifetime.

Most studies of blue emitters have tested molecules with excellent fluorescence characteristics such as anthracene, pyrene, and fluorine as single core or side moieties.[20–25] Many studies have investigated the use of anthracene and pyrene as the single cores of blue emitting materials since they have high PL efficiencies. In our previous study, the blue emissions of many anthracene derivatives with a single core moiety were investigated.[26–28] We synthesized and investigated new blue emitting materials that have symmetric or asymmetric chemical structures with bulky side groups, and in particular introduced anthracene as a single core and *m*-terphenyl and triphenylbenzene groups as side groups based on a core-side concept.[26] In addition, we investigated the electroluminescence properties that arise when diphenylamine and triphenylamine side groups are attached to the core, which means that there is electron donation in the emitter that occurs from the side groups to the core moiety.[27] To determine the effects of varying the positions of the links between the core and the side groups, we showed that the link position could be changed into *ortho*, *meta* and *para* to change emission wavelengths and strengthen emission efficiency according to the position of a side group.[29]

[a]*Department of Chemistry, The Catholic University of Korea, Bucheon, 420-743, South Korea. E-mail: hahapark@catholic.ac.kr; Fax: +82 2 2164 4764; Tel: +82 2 2164 4821*

[b]*Department of Polymer Science and Engineering & Department of IT Convergence, Korea National University of Transportation, Chungju, 380-702, South Korea. E-mail: jihoonli@ut.ac.kr; Fax: +82 43 841 5420; Tel: +82 43 841 5427*

† Electronic supplementary information (ESI) available. See DOI: 10.1039/c4tc00075g

‡ Hayoon Lee and Beomjin Kim contributed equally to this work.

Moreover, we recently reported the syntheses of new dual core chromophore materials containing anthracene and pyrene that exhibit high PL efficiencies.[30] There is a dihedral angle of approximately 90° between the two chromophores in a dual core composed of anthracene and pyrene. Compounds based on dual cores have advantages such as the prevention of excimer formation and improvements in the efficiency and lifetime of devices. However, there has been a lack of research into such dual core materials; no systematic study of the substitution of side groups onto dual cores has previously been performed.

In this study, we introduced phenyl and naphthyl groups onto various positions of dual cores in order to investigate the changes in the efficiencies of the first and the second core moieties. The newly synthesized compounds are blue emitting materials that have asymmetric or symmetric structures and that exhibit high efficiencies. The underlying dual core of the newly synthesized compounds is 1-anthracen-9-yl-pyrene (AP-core). The asymmetric structures 1-naphthalen-1-yl-6-(10-phenyl-anthracen-9-yl)-pyrene (Ph-AP-Na) and 1-(10-naphthalen-1-yl-anthracen-9-yl)-6-phenyl-pyrene (Na-AP-Ph), and the symmetric structures 1-phenyl-6-(10-phenyl-anthracen-9-yl)-pyrene (Ph-AP-Ph) and 1-naphthalen-1-yl-6-(10-naphthalen-1-yl-anthracen-9-yl)-pyrene (Na-AP-Na) were synthesized. The thermal and electro-optical properties of these materials were characterized by using differential scanning calorimetry (DSC), thermogravimetric analysis (TGA), as well as ultraviolet-visible (UV-vis) and photoluminescence (PL) spectroscopies. Multilayered EL devices were fabricated with these materials as non-doped emitting layers.

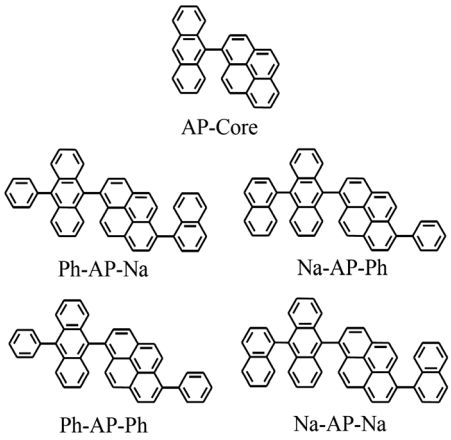

Scheme 1 Chemical structures of the new blue emitting materials.

Results and discussion

Synthesis and optical properties

Scheme 1 shows the chemical structures of the synthesized compounds. Ph-AP-Na and Na-AP-Ph have asymmetric chemical structures and Ph-AP-Ph and Na-AP-Na have some symmetry. A dual core mainly consisted of anthracene and pyrene groups and a side group was used with phenyl and naphthyl groups. All compounds were purified with reprecipitation and the column chromatography method. The synthesized compounds were characterized by using nuclear magnetic resonance (NMR) spectroscopy, elemental analysis, and FAB mass analysis. All the synthesis methods are shown in Scheme 2. Boronylation, bromination, and Suzuki aryl–aryl coupling reactions were used in the syntheses. The synthesis methods are described in more detail in the Experimental section.

The optical properties of the synthesized compounds are summarized in Table 1. The absorption peak wavelengths of synthesized compounds, AP-core, Ph-AP-Na, Na-AP-Ph, Ph-AP-Ph and Na-AP-Na in the solution and film state appear in the range of 350 to 400 nm.

According to the HOMO and LUMO electron density distributions of the AP-core, more electrons are located in anthracene than in pyrene (Fig. 1). However, the electron densities of HOMO−1 and LUMO+1 indicate that many electrons are distributed in pyrene. It means that the main electron transfer from the excited state to the ground state after excitation can first occur at the anthracene moiety. When the electron density distribution of Ph-AP-Na, Na-AP-Ph, Ph-AP-Ph and Na-AP-Na is considered, it is almost the same (Fig. S1†). It can be seen that anthracene and pyrene function as the first and second cores respectively in AP-core derivatives.

This conclusion is supported by the results of the time-dependent density functional theory (TD-DFT) calculations in Table 2. The HOMO → LUMO transition and the HOMO−1 → LUMO transition are respectively 71.8% and 17.1% at 390 nm, which has the highest oscillator strength of the AP-core. Accordingly, it can be seen that intramolecular charge transfer (ICT) arises from pyrene to anthracene and that pyrene functions as the second core. In the case of Na-AP-Na, the contributions of the HOMO → LUMO transition and the HOMO−1 → LUMO transition are 59.5% and 34.5% respectively at 400 nm, which has the highest oscillator strength, so the contribution of the HOMO−1 → LUMO transition is considerably greater than that in the other compounds.

In the case of Na-AP-Ph, the contributions of the HOMO → LUMO transition and the HOMO−1 → LUMO transition are 62.5% and 23.1% respectively at 399 nm, which has the highest oscillator strength, so the contribution of pyrene to the HOMO−1 → LUMO transition is still significant, even though it is smaller than that in Na-AP-Na. In the cases of Ph-AP-Na and Ph-AP-Ph, the contribution of the HOMO → LUMO transition is dominant and the contributions of the HOMO−1 → LUMO transition are respectively 5.5% and 6.7% at 399 nm, which has the greatest oscillator strength. Accordingly, it can be seen that the HOMO−1 → LUMO transition is made from pyrene even if its contribution is smaller than the other two compounds. Further, when the substituent of anthracene is changed from phenyl to naphthyl, the pyrene transition portion of the HOMO−1 → LUMO transition increases. Thus, anthracene and pyrene function effectively as dual cores because the HOMO−1 → LUMO transition occurs even though the HOMO → LUMO transition is dominant in all five compounds.

The relative PL quantum efficiencies (QEs and Φ_f) of the synthesized compounds in the solution state were determined as described previously.[26,31]

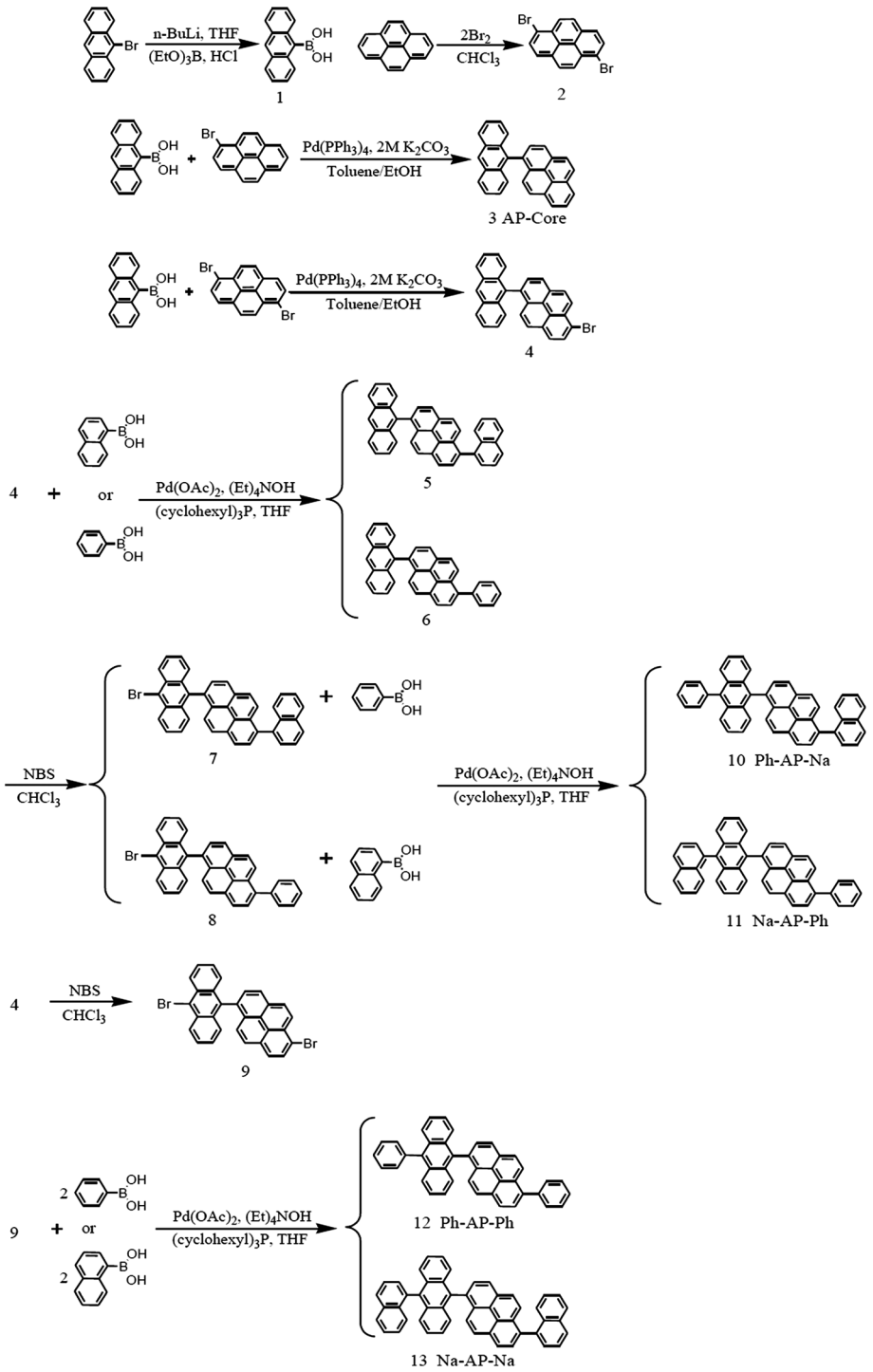

Scheme 2 Synthetic routes for the AP-core, Ph-AP-Na, Na-AP-Ph, Ph-AP-Ph, and Na-AP-Na.

$$\Phi_{F(A)} = \Phi_{F(ref)} \times \frac{PL_A}{UV_A} \times \frac{UV_{ref}}{PL_{ref}} \times \left(\frac{\eta_A}{\eta_{ref}}\right)^2 \quad (1)$$

$\Phi_{F(A)}$ is the relative Φ_F of the five synthesized compounds in $CHCl_3$ solution. Here, $\Phi_{F(ref)} = 0.91$ (QE in ethanol solution of 9,10-diphenylanthracene) was used. PL_A and PL_{ref} are the integrated emission intensities of the sample and the standard respectively. UV_A and UV_{ref} are the absorbances of the sample and the standard at the excitation wavelength respectively, and η_A and η_{ref} are the refractive indices of the corresponding solvents (pure solvents were assumed). The QEs of the five compounds were compared, as shown in Table 1. The QE of the AP-core is 0.76. Ph-AP-Na, Na-AP-Ph, Ph-AP-Ph, and Na-AP-Na have QEs between 0.85 and 0.96. Na-AP-Na has the highest value, 0.96.

The PL maximum values of the five compounds were compared. The PL maximum of the AP-core is 434 nm in the

Table 1 Optical, electrical, and thermal properties of the synthesized compounds

	Solution[a]			Film on glass								
Compounds	λ_{max}^{ab} (nm)	λ_{max}^{em} (nm)	FWHM[b] (nm)	λ_{max}^{ab} (nm)	λ_{max}^{em} (nm)	FWHM[b] (nm)	Φ_f[c]	HO MO[d] (eV)	LU MO (eV)	Band gap (eV)	T_g (°C)	T_d (°C)
AP-core	330, 343, 369, 389	434	59	337, 352, 375, 396	453	75	0.76	−5.75	−2.77	2.98	92	329
Ph-AP-Na	354, 378, 399	442	55	363, 382, 404	451	60	0.95	−5.75	−2.84	2.91	256	432
Na-AP-Ph	359, 378, 399	444	57	364, 382, 404	453	63	0.85	−5.71	−2.77	2.94	181	432
Ph-AP-Ph	358, 378, 399	443	56	364, 382, 404	450	59	0.92	−5.78	−2.82	2.96	228	439
Na-AP-Na	358, 378, 399	443	56	363, 382, 404	450	58	0.96	−5.78	−2.87	2.91	218	450

[a] $CHCl_3$ solution (1.00×10^{-5} M). [b] Full width at half maximum. [c] Relative photoluminescence efficiency in $CHCl_3$ solution using 9,10-diphenylanthracene as the reference (absolute photoluminescence efficiency, $\Phi_f = 0.91$ in EtOH). [d] Ultraviolet photoelectron spectroscopy (Riken-Keiki, AC-2).

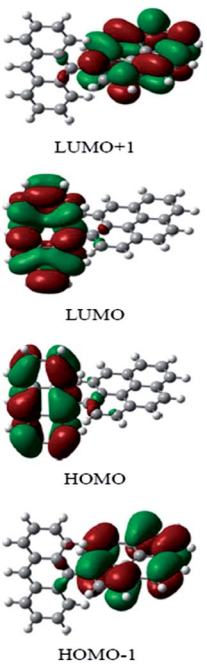

Fig. 1 Electron density distributions of HOMO−1, HOMO, LUMO and LUMO+1 in the AP-core calculated with B3LYP/6-311G(d).

solution state, whereas those of the other compounds lie between 442 and 444 nm, *i.e.* a 10 nm shift with respect to that of the AP-core. This shift can be explained by the extended conjugation lengths of the phenyl and naphthyl groups of anthracene, which are similar to those of conventional single core compounds based on anthracene.[26] The PL maximum values of the four synthesized compounds with side groups are similar because there are no special dipole moieties in the side groups. The five compounds exhibit similar PL maximum values in the film state, between 450 and 453 nm. In the film state, the phenyl and naphthyl side groups have no clear effect on the PL maxima. Although the pyrene group is directly connected to the anthracene group in the core, this connection does not affect the conjugation length significantly or the PL maximum value because anthracene and pyrene, the two chromophores in the AP-core, are orthogonally connected at an angle of 93.2°; this orthogonal structure prevents conjugation and any red-shift in the PL maximum value (Fig. 2).

According to the FWHM results for Ph-AP-Na, Na-AP-Ph, Ph-AP-Ph, and Na-AP-Na, the presence of a side group results in slight decreases by 2 to 4 nm in the solution state and large decreases by 12 to 17 nm in the film state compared to the results for the AP-core. These decreases arise because packing is prevented by the side groups. The FWHMs for the film state are higher than those for the solution state because the spectrum becomes broader when the molecules pack in the film state, which is tighter than packing in the solution state. In the case of the AP-core, the increase in the value of the FWHM is 16 nm, whereas the increases for Ph-AP-Na, Na-AP-Ph, Ph-AP-Ph, and Na-AP-Na are in the range 2 to 6 nm. In other words, the FWHM values of Ph-AP-Na, Na-AP-Ph, Ph-AP-Ph, and Na-AP-Na decrease by 10 nm or more compared with that of the AP-core. Thus, the EL device color coordinates of the four compounds are expected to be superior to the color coordinates of the AP-core in the blue region because their FWHM values are less than that of the AP-core. The UV-vis absorption and PL patterns of the five compounds are similar on the whole regardless of whether phenyl or naphthyl side groups are present (Fig. 3).

Electrochemical and thermal properties

The highest occupied molecular orbital (HOMO) levels were determined by photoelectron spectroscopy by using an ultraviolet light energy source. The lowest unoccupied molecular orbital (LUMO) energy levels were obtained from the HOMO levels and the optical band gaps (Table 1). The optical band gaps were derived by determining the absorption edges from plots of $(h\nu)$ *vs.* $(\alpha h\nu)^2$, where α, h, and ν are the absorbance, Planck's constant, and the frequency of light, respectively. The HOMO

Table 2 Absorption frequencies and oscillator strengths calculated with TD-B3LYP/6-311G(d) for the AP-core, Ph-AP-Na, Na-AP-Ph, Ph-AP-Ph, and Na-AP-Na

Compounds	Wavelength (nm)	Oscillator strength	Characteristic of transition	Contribution[a] (%)
AP-core	397	0.0327	HOMO−1 → LUMO	48.3
			HOMO → LUMO	25.1
			HOMO → LUMO+1	25.6
	395	0.0007	HOMO−1 → LUMO	33.4
			HOMO → LUMO+1	65.7
	390	0.1262	HOMO−1 → LUMO	17.1
			HOMO−1 → LUMO+1	2.5
			HOMO → LUMO	71.8
			HOMO → LUMO+1	7.0
Ph-AP-Na	405	0.0009	HOMO → LUMO+1	99.1
	399	0.2637	HOMO−1 → LUMO	5.5
			HOMO−1 → LUMO+1	2.1
			HOMO → LUMO	90.7
	398	0.0162	HOMO−1 → LUMO	93.6
			HOMO → LUMO	5.3
Na-AP-Ph	407	0.0414	HOMO−1 → LUMO	3.9
			HOMO → LUMO	18.6
			HOMO → LUMO+1	76.0
	405	0.0339	HOMO−1 → LUMO	70.4
			HOMO → LUMO	14.5
			HOMO → LUMO+1	14.3
	399	0.2434	HOMO−1 → LUMO	23.1
			HOMO−1 → LUMO+1	5.9
			HOMO → LUMO	62.5
			HOMO → LUMO+1	6.9
Ph-AP-Ph	408	0.0031	HOMO → LUMO+1	97.7
	403	0.0140	HOMO−1 → LUMO	92.2
			HOMO → LUMO	6.6
	399	0.2863	HOMO−1 → LUMO	6.7
			HOMO−1 → LUMO+1	3.7
			HOMO → LUMO	87.4
Na-AP-Na	405	0.0103	HOMO → LUMO	4.1
			HOMO → LUMO+1	94.8
	400	0.1848	HOMO−1 → LUMO	34.5
			HOMO → LUMO	59.5
			HOMO → LUMO+1	3.5
	399	0.1078	HOMO−1 → LUMO	64.1
			HOMO → LUMO	32.1

[a] Contribution (%) = (coefficient)^2 × 2 × 100.

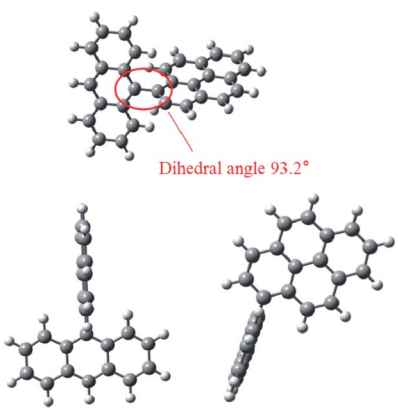

Fig. 2 Molecular structure of the AP-core optimized with B3LYP/6-311G(d).

and LUMO levels of the synthesized compounds were found to be in the ranges −5.71 to −5.78 eV and −2.77 to −2.87 eV respectively.

The glass transition temperatures (T_g) and the decomposition temperatures (T_d) of the synthesized compounds were determined with DSC and TGA respectively, and are summarized in Table 1. The T_g of the AP-core is 92 °C. The T_g values of Ph-AP-Na, Na-AP-Ph, Ph-AP-Ph, and Na-AP-Na are 256 °C, 181 °C, 228 °C, and 218 °C, respectively, approximately 100 °C to 150 °C higher than that of the AP-core. The T_d values of the AP-core, Ph-AP-Na, Na-AP-Ph, Ph-AP-Ph, and Na-AP-Na are 329 °C, 432 °C, 432 °C, 439 °C, and 450 °C, respectively. Note that these high T_g and T_d values indicate that the thermal properties of the compounds containing side groups are excellent; this improvement in thermal properties over those of the AP-core could be due to their increased molecular weights. In general, the thermal properties of films used in OLEDs are strongly

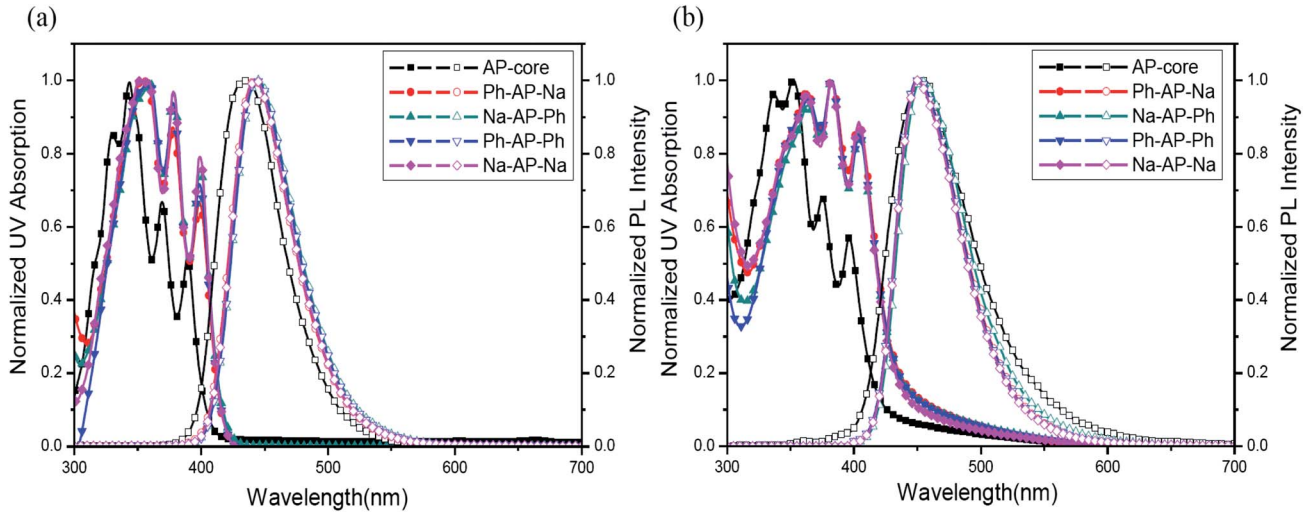

Fig. 3 UV-visible absorption spectra and PL spectra of the synthesized materials: (a) in $CHCl_3$ solution (1.00×10^{-5} M) and (b) in the thin film state.

associated with the device lifetime because Joule heating arises during device operation.[32] Therefore, devices containing these dual core materials with side groups are expected to exhibit long lifetimes under operation.

Fig. 4 shows surface atomic force microscopy (AFM) images of films of the dual core derivatives: obtained immediately after vacuum deposition (Fig. 4(a)) and after storage for 1 day at 100 °C under an argon atmosphere (Fig. 4(b)). Immediately after deposition, the root mean square (RMS) roughness values of the films of the AP-core, Ph-AP-Na, Na-AP-Ph, Ph-AP-Ph and Na-AP-Na were 0.3 nm, 0.6 nm, 0.3 nm, 0.4 nm, and 0.6 nm, respectively. The AP-core film has an RMS value of 43.2 nm after 1 day at 100 °C under an argon atmosphere, which is 144 times higher than that obtained immediately after vapor deposition.

However, the four compounds with side groups do not undergo any changes due to heat annealing; in fact, their RMS values are improved by this process. Examination of the AFM results shows that the dual core compounds with side groups have excellent characteristics after thermal annealing treatment. This result can be explained in terms of the high T_g and T_d values mentioned above.

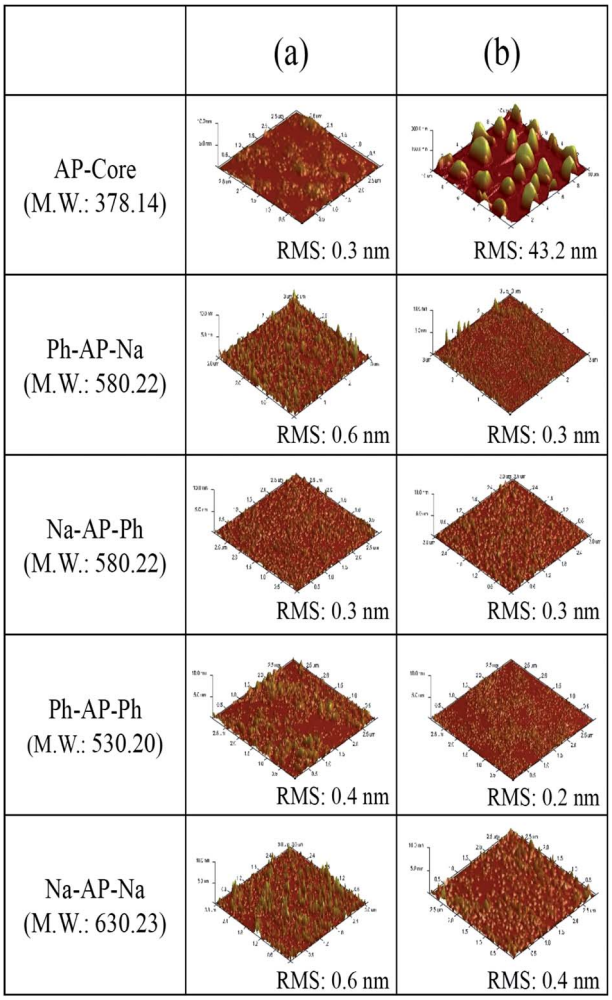

Fig. 4 AFM images of the AP-core, Ph-AP-Na, Na-AP-Ph, Ph-AP-Ph, and Na-AP-Na: (a) obtained immediately after evaporation and (b) after treatment at 100 °C for 1 day in an argon atmosphere.

Electroluminescence and thermal properties

The synthesized compounds were used as non-doped emitting layers (EMLs) in OLEDs with the following structures: ITO/2-TNATA (60 nm)/NPB (15 nm)/synthesized compound (35 nm)/Alq_3 (20 nm)/LiF (1 nm)/Al (200 nm). The OLED properties are summarized in Fig. 5 and Table 3.

The EL maximum values of the AP-core, Ph-AP-Na, Na-AP-Ph, Ph-AP-Ph, and Na-AP-Na devices are between 455 and 463 nm. While the FWHM value of the EL of the AP-core is 77 nm, those of Ph-AP-Na, Na-AP-Ph, Ph-AP-Ph, and Na-AP-Na are in the range 57 to 62 nm, which is 15 to 20 nm narrower than the value for the AP-core. This difference is similar to the result for the PL FWHM in the film state and the overall EL spectra are similar (Table 3 and Fig. 5(a)).

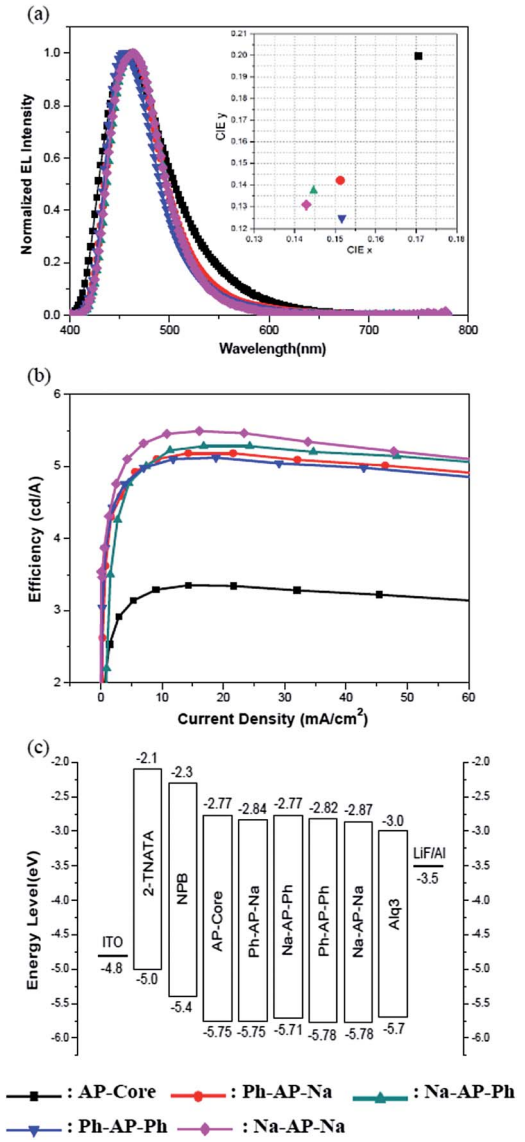

Fig. 5 EL characteristics of devices using the synthetic materials as EMLs: (a) EL spectra and CIE diagram, (b) luminance efficiency *versus* current density, and (c) energy diagrams of the compounds.

The AP-core device has an efficiency of 3.34 cd A^{-1} but the luminance efficiencies of the devices containing the four compounds with side groups are higher, between 5.11 and 5.46 cd A^{-1}. This increase in efficiency can be explained in terms of the higher PL efficiency of the four compounds and the lower energy transfer loss that arises because of the decreased molecular packing with respect to that of the AP-core due to their side groups. Fig. 5(b) clearly shows the difference between the luminance efficiencies of the core compound and the core-side compounds. As shown in Fig. 5(c), the LUMO levels of Ph-AP-Na, Na-AP-Ph, Ph-AP-Ph, and Na-AP-Na are similar and are in the range −2.77 to −2.87 eV. The differences between these LUMO levels and the LUMO level of Alq_3 (used as the electron transporting layer (ETL)) are small, in the range 0.23 to 0.13 eV, which means that the injection of electrons is facile. Therefore, the charge carrier balance is considered to be good.

We now analyze the luminance efficiency data more closely. Note that Ph-AP-Na and Ph-AP-Ph, in which the anthracene core is substituted with phenyl groups, have similar efficiencies, 5.18 cd A^{-1} and 5.11 cd A^{-1}. Ph-AP-Na has an efficiency slightly greater than that of Ph-AP-Ph. In Na-AP-Ph and Na-AP-Na, the anthracene core is substituted with naphthyl groups; the luminance efficiencies of these compounds are 5.28 cd A^{-1} and 5.46 cd A^{-1} respectively, which are higher than those of Ph-AP-Na and Ph-AP-Ph. The value for Na-AP-Na is the highest efficiency of the synthesized compounds. Therefore, the substitution of naphthyl at the anthracene core (the first core) improves the efficiency more than the substitution of phenyl. Also, the substitution of naphthyl at the second core of pyrene can improve the luminescence efficiency compared to phenyl substitution. The fact that Na-AP-Na has the highest luminance efficiency of this series of compounds coincides with the relative PL efficiency data shown in Table 1.

However, the order of the compounds in terms of EL efficiency does not exactly match that in terms of PL efficiency. Several factors may account for this observation, including charge transporting properties, HOMO and LUMO electronic levels, and charge balance of holes and electrons in the device. *I–V* and *L–V* curves are shown in Fig. S3;† however, these curves were obtained from devices that were not fully optimized for each compound. Further studies are underway to clarify this issue.

According to the CIE data, AP-core, Ph-AP-Na, Na-AP-Ph, Ph-AP-Ph, and Na-AP-Na have similar color coordinates. However, the FWHM of the AP-core is 77 nm, which is larger than those of the other compounds. This trend is the same as obtained for the PL FWHMs in the film state, and it indicates that packing is prevented by the side groups. As a result, the color coordinates of the AP-core are (0.170, 0.200); this *y* value is not satisfactory for blue color applications. In contrast, the coordinates for the dual core compounds with side groups Ph-AP-Na, Na-AP-Ph, Ph-AP-Ph, and Na-AP-Na are (0.151, 0.142), (0.144, 0.137), (0.152, 0.125), and (0.143, 0.131), respectively, which are good *x* and *y*

Table 3 ITO/2-TNATA (60 nm)/NPB (15 nm)/EML (35 nm)/Alq_3 (20 nm)/LiF (1 nm)/Al (200 nm)/at 20 mA cm^{-2}

Emitting material (EML)	Operating voltage (V)	EL_{max} (nm)	FWHM (nm)	Luminance efficiency (cd A^{-1})	Power efficiency (lm W^{-1})	CIE (*x*, *y*)
AP-core	7.77	460	77	3.34	1.46	(0.170, 0.200)
Ph-AP-Na	8.39	461	62	5.18	2.15	(0.151, 0.142)
Na-AP-Ph	8.86	463	60	5.28	2.11	(0.144, 0.137)
Ph-AP-Ph	7.56	455	57	5.11	2.35	(0.152, 0.125)
Na-AP-Na	9.27	463	62	5.46	2.05	(0.143, 0.131)

color coordinates in the blue region. Blue emitters require a *y* CIE coordinate value of less than 0.16 for the large color gamut of mobile displays and tablet PC applications, according to the National Television System Committee (NTSC) blue color standard (0.14, 0.08).

Further, we measured the average lifetimes of the synthesized compound devices at 1000 cd m^{-2}. The lifetime of the AP-core device is 91 h. In contrast, the lifetimes of the Ph-AP-Na, Na-AP-Ph, Ph-AP-Ph, and Na-AP-Na devices are 170 h, 305 h, 215 h, and 298 h, respectively, which are approximately 1.9 to 3.4 times longer than that of the AP-core device. These increased lifetimes are due to their high luminance efficiencies and excellent thermal properties. A high luminance efficiency means that the current density is smaller and that less Joule heating occurs for the same device brightness. The excellent thermal properties of these compounds mean that they are more robust than the AP-core under given heating conditions.

Conclusions

Five new dual core derivatives with high PL efficiencies based on anthracene and pyrene moieties, AP-core, Ph-AP-Na, Na-AP-Ph, Ph-AP-Ph, and Na-AP-Na, were synthesized and their electrical properties were characterized. Four of the dual core compounds contain side groups with systematic variation in size and substitution position. The dihedral angle between the two core chromophores of the AP-core is 93.2°, which prevents the lengthening of the conjugation. As a result, the UV-visible absorption peak and the PL emission peak are nearly identical.

The efficiency of the AP-core can be improved by substituting its large naphthyl component with the first core anthracene and the second core pyrene. Na-AP-Na exhibits a high luminance efficiency, 5.46 cd A^{-1}, in a non-doped device and good color coordinates of (0.143, 0.131) that are applicable to displays requiring a blue emitter. Thus an orthogonally connected dual core can be used to produce a blue emission spectrum and prepare blue emitting materials. The side groups can be varied to strengthen the EL efficiency. The FWHM values of Ph-AP-Na, Na-AP-Ph, Ph-AP-Ph, and Na-AP-Na are 15 to 20 nm narrower than the value for the AP-core. The dual core compounds with side groups have excellent characteristics such as high T_g and T_d values compared to the AP-core. The lifetime of the Na-AP-Na device was more than three times longer than the AP-core device.

Moreover, by introducing chromophores other than anthracene and pyrene, many different dual core systems can be prepared. In addition to side groups composed of aromatic rings, electron-donating or electron-withdrawing groups could be substituted to improve OLED device performance.

Experimental

General information

The ^{1}H-NMR spectra and ^{13}C-NMR spectra were recorded on Bruker Avance 300 and Avance 500 spectrometers. The FAB^+-mass and EI^+-spectra were recorded on a JEOL, JMS-AX505WA, HP5890 series II. The optical absorption spectra were obtained by using a Lambda 1050 UV/Vis/NIR spectrometer (PerkinElmer). A PerkinElmer luminescence spectrometer LS50 (xenon flash tube) was used to perform photoluminescence (PL) spectroscopy. The glass-transition temperatures (T_g) of the compounds were determined with differential scanning calorimetry (DSC) under a nitrogen atmosphere by using a DSC4000 (PerkinElmer). Samples were heated to 360 or 400 °C at a rate of 10 °C min^{-1} and cooled at 10 °C min^{-1} then heated again under the same heating conditions as used in the initial heating process. Degradation temperatures (T_d) were determined with thermogravimetric analysis (TGA) by using a TGA4000 (PerkinElmer). Samples were heated to 800 °C at a rate of 10 °C min^{-1}.

The HOMO energy levels were determined with ultraviolet photoelectron yield spectroscopy (Riken Keiki AC-2). The LUMO energy levels were derived from the HOMO energy levels and the band gaps. Atomic force microscopy (AFM) was performed in the tapping-mode by using a Multimode IIIa (Digital Instruments). The molecular structures were optimized by using time-dependent DFT (TD-DFT) on the optimized structures. In the TD-DFT calculations, the same exchange-correlation functional and basis sets were employed as used in the DFT calculations (TD-B3LYP/6-311G(d)). All DFT and TD-DFT calculations were performed with the Gaussian09 program.[33]

In each of the EL devices, tris(*N*-(naphthalen-2-yl)-*N*-phenylamino)triphenylamine (2-TNATA) was used for the hole injection layer (HIL), *N*,*N*′-bis(naphthalen-1-yl)-*N*,*N*′-bis(phenyl) benzidine (NPB) was used for the hole transporting layer (HTL), one of the synthetic materials AP-core, Ph-AP-Ph, Na-AP-Na, Ph-AP-Na, and Na-AP-Ph was used as the emitting layer (EML), 8-hydroxyquinoline aluminum (Alq_3) was used for the electron transporting layer (ETL), lithium fluoride (LiF) was used for the electron injection layer (EIL), and ITO was used as the anode and Al as the cathode. All organic layers were deposited under 10^{-6} Torr, with a rate of deposition of 1 Å s^{-1} to create an emitting area of 4 mm^2. The LiF and aluminum layers were continuously deposited under the same vacuum conditions. The luminance efficiency data for the fabricated EL devices were obtained by using a Keithley 2400 sourcemeter. Light intensities were obtained with a Minolta CS-1000A spectroradiometer. The operational stabilities of the devices were measured under encapsulation in a glove box. The device lifetimes were determined by using the Polaronix OLED Lifetime Test System of McScience.

Synthesis

Compound 1. 9-Bromoanthracence (10.0 g, 38.9 mmol) was dissolved in anhydrous THF solution (500 mL) and stirred at −78 °C. Then, 1.6 M *n*-BuLi (29.3 mL, 46.7 mmol) was added. Triethyl borate (9.3 mL, 54.5 mmol) was added to the reaction after 30 min. After the reaction had finished, the solution was acidified with 2 N HCl solution at room temperature and extracted with ethyl acetate and water. The organic layer was dried over anhydrous $MgSO_4$ and filtered. The solution was evaporated. The residue was re-dissolved in ethyl acetate and hexane was added into the solution. The precipitate was filtered and washed with hexane to obtain a beige compound (7.70 g,

89%). ^{1}H-NMR (300 MHz, $CDCl_3$, 25 °C, TMS): $\delta = 8.47$ (s, 1H), 8.14 (d, $J = 9.2$ Hz, 2H), 8.04 (d, $J = 9.8$ Hz, 2H), 7.53–7.44 (m, 4H), 5.07 ppm (s, 2H), EI$^+$-Mass: 222.

Compound 2. Bromine (10.0 mL, 194.7 mmol) in $CHCl_3$ (500 mL) was dropped into a solution of pyrene (20.0 g, 98.9 mmol) in $CHCl_3$ (500 mL) over 5 h while stirring. The precipitate was collected after 12 h and resolved by fractional crystallization from xylene (11.8 g, 33%). ^{1}H-NMR (300 MHz, $CDCl_3$, 25 °C, TMS): $\delta = 8.50$ (d, $J = 9.2$ Hz, 2H), 8.29 (d, $J = 8.2$ Hz, 2H), 8.16 (d, $J = 9.3$ Hz, 2H), 8.09 ppm (d, $J = 8.2$ Hz, 2H), EI$^+$-Mass: 360.

Compound 3 (AP-core). **1** (0.47 g, 2.12 mmol), 1-bromopyrene (0.50 g, 1.78 mmol), and $Pd(PPh_3)_4$ (0.103 g, 0.089 mmol) were added to anhydrous toluene solution (50.0 mL). Then, 2 M K_2CO_3 solution (7.0 mL) dissolved in H_2O was added to the reaction mixture at 50 °C after pouring anhydrous ethanol (20.0 mL) into the mixture. The mixture was heated to 65 °C for 4 h under nitrogen. After the reaction had finished, the reaction mixture was extracted with toluene and water. The organic layer was dried over anhydrous $MgSO_4$ and filtered. The solution was evaporated. The product was isolated with silica gel column chromatography by using CH_2Cl_2–*n*-hexane (1 : 7) as the eluent to afford a beige solid (0.50 g, 74%). ^{1}H-NMR (300 MHz, [D_8] THF): $\delta = 8.70$ (s, 1H), 8.44 (d, $J = 7.8$ Hz, 1H), 8.29 (d, $J = 8.7$ Hz, 2H), 8.23 (d, $J = 9.0$ Hz, 1H), 8.17 (d, $J = 9.6$ Hz, 3H), 8.04–7.99 (m, 2H), 7.80 (d, $J = 9.0$ Hz, 1H), 7.47 (t, $J = 6.6$ Hz, 2H), 7.32 (d, $J = 7.8$ Hz, 2H), 7.26 (d, $J = 9.0$ Hz, 1H), 7.22 ppm (t, $J = 6.3$ Hz, 2H); ^{13}C-NMR (300 MHz, $CDCl_3$, 25 °C, TMS): $\delta = 135.53$, 134.12, 131.66, 131.49, 131.28, 130.99, 129.58, 128.68, 127.94, 127.88, 127.71, 127.27, 127.23, 126.33, 125.91, 125.83, 125.47, 125.44, 125.38, 125.12, 125.03, 124.91 ppm; HRMS (EI, *m*/*z*): [M^+] calcd for $C_{30}H_{18}$, 378.1409; found, 378.1414. Anal. calcd for $C_{30}H_{18}$: C 95.21, H 4.79; found: C 95.21, H 4.73%.

Compound 4. **1** (4.0 g, 18.0 mmol), **2** (9.7 g, 27.0 mmol), and $Pd(PPh_3)_4$ (0.62 g, 0.54 mmol) were added to anhydrous toluene solution (150.0 mL) and anhydrous ethanol (8.0 mL). Then, 2 M K_2CO_3 solution (15.0 mL) dissolved in H_2O was added to the reaction mixture at 50 °C after pouring anhydrous ethanol (8.0 mL) into the mixture. The mixture was heated to 65 °C for 5 h under nitrogen. After the reaction had finished, the reaction mixture was extracted with toluene and water. The organic layer was dried over anhydrous $MgSO_4$ and filtered. The solution was evaporated. The product was isolated with silica gel column chromatography by using CH_2Cl_2–*n*-hexane (1 : 7) as the eluent to afford a beige solid (3.9 g, 32%). ^{1}H-NMR (300 MHz, $CDCl_3$, 25 °C, TMS): $\delta = 8.65$ (s, 1H), 8.58 (d, $J = 9.3$ Hz, 1H), 8.43 (d, $J = 7.8$ Hz, 1H), 8.34 (d, $J = 9.3$ Hz, 1H), 8.26 (d, $J = 8.4$ Hz, 1H), 8.15 (d, $J = 8.4$ Hz, 2H), 8.08 (d, $J = 7.8$ Hz, 1H), 7.95 (d, $J = 8.1$ Hz, 1H), 7.75 (d, $J = 9.0$ Hz, 1H), 7.49 (t, $J = 6.3$ Hz, 2H), 7.35 (t, $J = 9.0$ Hz, 3H), 7.24 ppm (t, $J = 6.3$ Hz, 2H), EI$^+$-Mass: 457.

Compound 5. This compound was synthesized with the same method as for compound **6** by using 1-naphthalene boronic acid (0.57 g, 3.31 mmol). A beige solid (0.70 g, 63%) was obtained. ^{1}H-NMR (300 MHz, [D_8]THF): $\delta = 8.72$ (s, 1H), 8.41 (d, $J = 7.8$ Hz, 1H), 8.29 (d, $J = 7.8$ Hz, 1H), 8.19 (d, $J = 8.5$ Hz, 2H), 8.09–8.01 (m, 5H), 7.92 (d, $J = 9.0$ Hz, 1H), 7.73–7.62 (m, 3H), 7.50–7.43 (m, 3H), 7.39–7.29 (m, 5H), 7.25–7.20 ppm (m, 2H). EI$^+$-Mass: 504.

Compound 6. **4** (1.0 g, 2.19 mmol), phenyl boronic acid (0.44 g, 3.61 mmol), $Pd(OAC)_2$ (0.02 g, 0.09 mmol), and $(cyclohexyl)_3P$ (0.04 g, 0.14 mmol) were added to anhydrous THF (100.0 mL) solution. Then tetraethylammonium hydroxide (20 wt%) (10.0 mL) was added to the reaction mixture at 50 °C. The mixture was heated to 80 °C for 2 h under nitrogen. After the reaction had finished, the reaction mixture was extracted with $CHCl_3$ and water. The organic layer was dried over anhydrous $MgSO_4$ and filtered. The solution was evaporated. The residue was re-dissolved in $CHCl_3$ and added to ethanol. The precipitate was filtered and washed with ethanol. The yellow powder was purified by using column chromatography with CH_2Cl_2–*n*-hexane (1 : 7) as the eluent to afford a white solid (0.70 g, 70%). ^{1}H-NMR (300 MHz, $CDCl_3$, 25 °C, TMS): $\delta = 8.65$ (s, 1H), 8.37 (d, $J = 7.8$ Hz, 1H), 8.30 (d, $J = 9.3$ Hz, 1H), 8.19–8.13 (m, 4H), 8.05 (d, $J = 7.8$ Hz, 1H), 8.01 (d, $J = 7.8$ Hz, 1H), 7.83 (d, $J = 9.2$ Hz, 1H), 7.69 (d, $J = 8.3$ Hz, 2H), 7.62 (t, $J = 7.05$ Hz, 2H), 7.53–7.44 (m, 3H), 7.38 (t, $J = 8.9$ Hz, 3H), 7.23 ppm (d, $J = 9.1$ Hz, 2H), EI$^+$-Mass: 454.

Compound 7. This compound was synthesized with the same method as for compound **8** by using **5** (0.7 g, 1.38 mmol). Accordingly, a yellow solid (0.28 g, 34%) was obtained. ^{1}H-NMR (300 MHz, $CDCl_3$, 25 °C, TMS): $\delta = 8.73$ (dd, $J = 8.9$ Hz, 2H), 8.34 (d, $J = 7.8$ Hz, 1H), 8.24 (d, $J = 7.9$ Hz, 1H), 8.05 (t, $J = 7.8$ Hz, 5H), 7.90 (d, $J = 9.2$ Hz, 1H), 7.80 (d, $J = 9.1$ Hz, 1H), 7.72–7.50 (m, 6H), 7.45–7.23 ppm (m, 6H). EI$^+$-Mass: 582.

Compound 8. **6** (0.70 g, 1.53 mmol) and *N*-bromosuccinimide (NBS) (0.30 g, 1.68 mmol) were added to $CHCl_3$ (50.0 mL), and acetic acid (1.0 mL) was added to the reaction mixture. The mixture was refluxed for 3 h. After the reaction had finished, the reaction mixture was extracted with $CHCl_3$ and water. The organic layer was dried over anhydrous $MgSO_4$ and filtered. The solution was evaporated. The residue was re-dissolved in acetone and added to $CHCl_3$. The precipitate was filtered and washed with acetone to obtain a yellow compound (0.23 g, 28%). ^{1}H-NMR (300 MHz, $CDCl_3$, 25 °C, TMS): $\delta = 8.72$ (d, $J = 8.9$ Hz, 2H), 8.38 (d, $J = 8.34$ Hz, 1H), 8.32 (d, $J = 8.8$ Hz, 1H), 8.19 (d, $J = 10.7$ Hz, 2H), 8.02 (dd, $J = 7.7$ Hz, 2H), 7.84 (d, $J = 9.1$ Hz, 1H), 7.69 (d, $J = 6.0$ Hz, 2H), 7.63 (t, $J = 7.7$ Hz, 4H), 7.54 (t, $J = 7.2$ Hz, 1H), 7.38 (d, $J = 8.7$ Hz, 2H), 7.31–7.22 ppm (m, 3H). EI$^+$-Mass: 532 [M^+].

Compound 9. **4** (1.0 g, 2.19 mmol) and *N*-bromosuccinimide (NBS) (0.43 g, 2.41 mmol) were added to $CHCl_3$ (30.0 mL) and acetic acid (5.0 mL) was added to the reaction mixture. The mixture was refluxed for 2 h. After the reaction had finished, the reaction mixture was extracted with $CHCl_3$ and water. The organic layer was dried over anhydrous $MgSO_4$ and filtered. The solution was evaporated. The residue was re-dissolved in ethanol and added to $CHCl_3$. The precipitate was filtered and washed with ethanol to obtain a yellow compound (1.1 g, 96%). ^{1}H-NMR (300 MHz, $CDCl_3$, 25 °C, TMS): $\delta = 8.71$ (d, $J = 8.1$ Hz, 2H), 8.60 (d, $J = 9.2$ Hz, 1H), 8.44 (d, $J = 7.8$ Hz, 1H), 8.35 (d, $J = 9.3$ Hz, 1H), 8.28 (d, $J = 8.2$ Hz, 1H), 8.06 (d, $J = 7.8$ Hz, 1H), 7.97 (d, $J = 8.3$ Hz, 1H), 7.77 (d, $J = 9.2$ Hz, 1H), 7.62 (t, $J = 6.3$ Hz, 2H), 7.33 (d, $J = 3.6$ Hz, 2H), 7.30 (d, $J = 5.3$ Hz, 1H), 7.26–7.24 ppm (m, 2H), EI$^+$-Mass: 536.

Compound 10 (Ph-AP-Na). **7** (1.0 g, 1.70 mmol), phenyl boronic acid (0.32 g, 2.62 mmol), $Pd(OAC)_2$ (0.02 g, 0.09 mmol),

and (cyclohexyl)$_3$P (0.05 g, 0.18 mmol) were added to anhydrous THF (100.0 mL) solution. Then tetraethylammonium hydroxide (20 wt%) (10.0 mL) was added to the reaction mixture at 50 °C. The mixture was heated to 80 °C for 2 h under nitrogen. After the reaction had finished, the reaction mixture was extracted with $CHCl_3$ and water. The organic layer was dried over anhydrous $MgSO_4$ and filtered. The solution was evaporated. The residue was re-dissolved in $CHCl_3$ and added to ethanol. The precipitate was filtered and washed with ethanol. The yellow powder was purified by using column chromatography with CH_2Cl_2–*n*-hexane (1 : 7) as the eluent to afford a beige solid (0.55 g, 55%). ^{1}H-NMR (300 MHz, [D$_8$]THF): δ = 8.44 (d, J = 7.8 Hz, 1H), 8.31 (d, J = 7.8 Hz, 1H), 8.11–8.02 (m, 5H), 7.96 (d, J = 9.3 Hz, 1H), 7.79 (d, J = 8.7 Hz, 2H), 7.74–7.50 (m, 9H), 7.42–7.29 (m, 7H), 7.23 ppm (t, J = 7.2 Hz, 2H); ^{13}C-NMR (300 MHz, $CDCl_3$, 25 °C, TMS): δ = 139.30, 139.11, 137.92, 136.46, 135.64, 134.65, 133.87, 133.30, 131.64, 131.41, 131.18, 131.02, 130.44, 130.23, 129.90, 128.89, 128.70, 128.64, 128.49, 128.29, 128.06, 127.79, 127.76, 127.39, 126.93, 126.39, 126.27, 126.15, 125.67, 125.53, 125.36, 125.26, 125.12, 125.07, 124.95 ppm; HRMS (EI, *m*/*z*): [M$^+$] calcd for $C_{46}H_{28}$, 580.2191; found, 580.2188. Anal. calcd for $C_{46}H_{28}$: C 95.14, H 4.86; found: C 95.15, H 4.90%.

Compound 11 (Na-AP-Ph). 8 (0.8 g, 1.50 mmol), 1-naphthalene boronic acid (0.39 g, 2.26 mmol), Pd(OAC)$_2$ (0.02 g, 0.09 mmol), and (cyclohexyl)$_3$P (0.04 g, 0.14 mmol) were added to anhydrous THF (50.0 mL) solution. Then tetraethylammonium hydroxide (20 wt%) (5.0 mL) was added to the reaction mixture at 50 °C. The mixture was heated to 80 °C for 2 h under nitrogen. After the reaction had finished, the reaction mixture was extracted with $CHCl_3$ and water. The organic layer was dried over anhydrous $MgSO_4$ and filtered. The solution was evaporated. The residue was re-dissolved in $CHCl_3$ and added to ethanol. The precipitate was filtered and washed with ethanol. The yellow powder was purified by using column chromatography with CH_2Cl_2–*n*-hexane (1 : 7) as the eluent to afford an ivory solid (0.48 g, 55%).^{1}H-NMR (300 MHz, [D$_8$]THF): δ = 8.50 (q, J = 6.3 Hz, 2H), 8.32 (d, J = 7.5 Hz, 2H), 8.27–8.23 (m, 4H), 8.19 (d, J = 7.5 Hz, 2H), 8.14 (t, J = 1.5 Hz, 2H), 8.09 (dd, J = 9.0 Hz, 2H), 8.04 (dd, J = 7.8 Hz, 2H), 7.96 (dd, J = 9.2 Hz, 2H), 7.96 (d, J = 9.6 Hz, 1H), 7.77 (d, J = 6.0 Hz, 1H), 7.72–7.62 (m, 7H), 7.60 (d, J = 7.8 Hz, 3H), 7.52–7.41 (m, 14H), 7.32–7.16 ppm (m, 12H); ^{13}C-NMR (300 MHz, $CDCl_3$, 25 °C, TMS): δ = 141.49, 138.39, 138.36, 136.99, 136.05, 135.79, 134.49, 133.98, 133.89, 131.49, 131.19, 130.96, 130.86, 130.75, 129.92, 129.85, 129.54, 129.49, 129.06, 128.65, 128.53, 128.49, 128.41, 128.13, 128.06, 127.79, 127.54, 127.44, 126.93, 126.62, 126.55, 126.30, 126.27, 126.06, 125.85, 125.58, 125.52, 125.41, 125.35, 125.14, 125.11, 124.85 ppm; HRMS (EI, *m*/*z*): [M$^+$] calcd for $C_{46}H_{28}$, 580.2191; found, 580.2195. Anal. calcd for $C_{46}H_{28}$: C 95.14, H 4.86; found: C 95.02, H 4.97%.

Compound 12 (Ph-AP-Ph). 9 (1.0 g, 1.9 mmol), phenyl boronic acid (0.7 g, 5.6 mmol), Pd(OAc)$_2$ (0.04 g, 0.19 mmol), and (cyclohexyl)$_3$P (0.13 g, 0.46 mmol) were added to anhydrous THF (100.0 mL) solution. Then, tetraethylammonium hydroxide (20 wt%) (10.0 mL) was added to the reaction mixture. The mixture was heated to 85 °C for 2 h under nitrogen. After the reaction had finished, the reaction mixture was extracted with $CHCl_3$ and water. The organic layer was dried over anhydrous $MgSO_4$ and filtered. The solution was evaporated. The residue was re-dissolved in $CHCl_3$ and added to ethanol. The precipitate was filtered and washed with ethanol. The yellowish powder was purified by using column chromatography with CH_2Cl_2–*n*-hexane (1 : 7) as the eluent to afford a beige solid (Ph-AP-Ph) (0.6 g, 59%). ^{1}H-NMR (500 MHz, $CDCl_3$, 25 °C, TMS): δ = 8.39 (d, J = 7.5 Hz, 1H), 8.30 (d, J = 9.5 Hz, 1H), 8.19 (d, J = 7.0 Hz, 1H), 8.17 (d, J = 5.5 Hz, 1H), 8.10 (d, J = 7.5 Hz, 1H), 8.01 (d, J = 8.0 Hz, 1H), 7.86 (d, J = 9.5 Hz, 1H), 7.80 (d, J = 9.0 Hz, 2H), 7.69–7.56 (m, 9H), 7.53 (t, J = 7.5 Hz, 1H), 7.45 (d, J = 9.5 Hz, 1H), 7.41 (d, J = 8.5 Hz, 2H), 7.35 (t, J = 6.5 Hz, 2H), 7.21 ppm (t, J = 7.5 Hz, 2H); ^{13}C-NMR (500 MHz, $CDCl_3$, 25 °C, TMS): δ = 141.30, 139.11, 138.14, 137.68, 135.47, 134.33, 131.43, 131.26, 130.96, 130.64, 130.54, 130.02, 129.65, 128.86, 128.46, 128.42, 127.88, 127.81, 127.56, 127.32, 127.16, 125.84, 125.61, 125.28, 125.18, 125.11, 124.86, 124.62 ppm; HRMS (EI, *m*/*z*): [M$^+$] calcd for $C_{42}H_{26}$, 530.2035; found, 530.2039. Anal. calcd for $C_{42}H_{26}$: C 95.06, H 4.94; found: C 95.03, H 4.98%.

Compound 13 (Na-AP-Na). 9 (1.0 g, 1.9 mmol), 1-naphthalene boronic acid (0.80 g, 4.65 mmol), Pd(OAc)$_2$ (0.04 g, 0.19 mmol), and (cyclohexyl)$_3$P (0.13 g, 0.46 mmol) were added to anhydrous THF (100.0 mL) solution. Then, tetraethylammonium hydroxide (20 wt%) (10.0 mL) was added to the reaction mixture. The mixture was heated to 85 °C for 2 h under nitrogen. After the reaction had finished, the reaction mixture was extracted with $CHCl_3$ and water. The organic layer was dried over anhydrous $MgSO_4$ and filtered. The solution was evaporated. The residue was re-dissolved in $CHCl_3$ and added to ethanol. The precipitate was filtered and washed with ethanol. The yellowish powder was purified by using column chromatography with CH_2Cl_2–*n*-hexane (1 : 7) as the eluent to afford a beige solid (0.60 g, 51%). ^{1}H-NMR (300 MHz, [D$_8$]THF): δ = 8.48 (q, J = 6.0 Hz, 2H), 8.34 (q, J = 6.0 Hz, 2H), 8.20 (d, J = 7.8 Hz, 2H), 8.15–8.12 (m, 3H), 8.10–7.96 (m, 11H), 7.83 (d, J = 9.0 Hz, 1H), 7.78 (t, J = 4.5 Hz, 4H), 7.73 (d, J = 5.7 Hz, 2H), 7.66 (d, J = 6.9 Hz, 3H), 7.56–7.39 (m, 16H), 7.33–7.17 ppm (m, 14H); ^{13}C-NMR (300 MHz, $CDCl_3$, 25 °C, TMS): δ = 139.11, 137.00, 136.52, 135.99, 135.80, 134.62, 134.00, 133.88, 133.30, 131.42, 131.23, 131.03, 130.98, 130.46, 129.97, 129.90, 129.50, 128.91, 128.65, 128.50, 128.44, 128.30, 128.17, 128.09, 127.78, 127.46, 126.94, 126.64, 126.57, 126.40, 126.30, 126.16, 125.88, 125.67, 125.63, 125.55, 125.30, 125.09, 125.01 ppm; HRMS (EI, *m*/*z*): [M$^+$] calcd for $C_{50}H_{30}$, 630.2347; found, 630.2345. Anal. calcd for $C_{50}H_{30}$: C 95.21, H 4.79; found: C 95.23, H 4.72%.

Acknowledgements

This work was supported by the National Research Foundation of Korea (NRF) grant funded by the Korea government (MEST) (no. 2012001846).

Notes and references

1 C. W. Tang and S. A. Vanslyke, *Appl. Phys. Lett.*, 1987, **51**, 913.

2 M. F. Wu, S. J. Yeh, C. T. Chen, H. Murayama, T. Tsuboi, W. S. Li, I. Chao, S. W. Liu and J. K. Wang, *Adv. Funct. Mater.*, 2007, **17**, 1887.
3 Z. Zhao, C. Deng, S. Chen, J. W. Y. Lam, W. Qin, P. Lu, Z. Wang, H. S. Kwok, Y. Ma, H. Qiu and B. Z. Tang, *Chem. Commun.*, 2011, **47**, 8847.
4 H. Wu, G. Zhou, J. Zou, C. L. Ho, W. Y. Wong, W. Yang, J. Peng and Y. Cao, *Adv. Mater.*, 2009, **21**, 4181.
5 M. C. Gather, A. Kohnen, A. Falcou, H. Becker and K. Meerholz, *Adv. Funct. Mater.*, 2007, **17**, 191.
6 J. Huang, X. Wang, A. J. deMello, J. C. deMello and D. D. C. Bradley, *J. Mater. Chem.*, 2007, **17**, 3551.
7 R. Capelli, S. Toffanin, G. Generali, H. Usta, A. Facchetti and M. Muccini, *Nat. Mater.*, 2010, **9**, 496.
8 Y. Yang, R. T. Farley, T. T. Steckler, S. H. Eom, J. R. Reynolds, K. S. Schanze and J. Xue, *J. Appl. Phys.*, 2009, **106**, 044509.
9 T. Tsuzuki and S. Tokito, *Adv. Mater.*, 2007, **19**, 276.
10 B. R. Lee, W. Lee, T. L. Nguyen, J. S. Park, J. S. Kim, J. Y. Kim, H. Y. Woo and M. H. Song, *ACS Appl. Mater. Interfaces*, 2013, **5**, 5690.
11 M. Cocchi, D. Virgili, V. Fattori, D. L. Rochester and J. A. G. Williams, *Adv. Funct. Mater.*, 2007, **17**, 285.
12 Y. Liu, S. Chen, J. W. Y. Lam, P. Lu, R. T. K. Kwok, F. Mahtab, H. S. Kwok and B. Z. Tang, *Chem. Mater.*, 2011, **23**, 2536.
13 J. You, S. L. Lai, W. Liu, T. W. Ng, P. Wang and C. S. Lee, *J. Mater. Chem.*, 2012, **22**, 8922.
14 J. K. Bin and J. I. Hong, *Org. Electron.*, 2012, **13**, 2893.
15 M. M. Rothmann, S. Haneder, E. D. Como, C. Lennartz, C. Schildknecht and P. Strohriegl, *Chem. Mater.*, 2010, **22**, 2403.
16 Y. I. Park, J. H. Son, J. S. Kang, S. K. Kim, J. H. Lee and J. W. Park, *Chem. Commun.*, 2008, 2143.
17 J. H. Ahn, C. Wang, I. F. Perepichka, M. R. Bryce and M. C. Petty, *J. Mater. Chem.*, 2007, **17**, 2996.
18 R. Ma, P. A. Levermore, A. Dyatkin, Z. Elshenawy, V. Adamovich, H. Pang, R. C. Kwong, M. S. Weaver, M. Hack and J. J. Brown, *IMID Dig.*, 2011, 60.
19 Y. Kawamura, H. Kuma, M. Funahashi, M. Kawamura, Y. Mizuki, H. Saito, R. Naraoka, K. Nishimura, Y. Jinde, T. Iwakuma and C. Hosokawa, *SID Dig.*, 2011, 829.
20 H. Park, J. Lee, I. Kang, H. Y. Chu, J. I. Lee, S. K. Kwon and Y. H. Kim, *J. Mater. Chem.*, 2012, **22**, 2695.
21 Z. Q. Wang, C. Xu, W. Z. Wang, L. M. Duan, Z. Li, B. T. Zhao and B. M. Ji, *New J. Chem.*, 2012, **36**, 662.
22 M. S. Gong, H. S. Lee and Y. M. Jeon, *J. Mater. Chem.*, 2010, **20**, 10735.
23 C. H. Wu, C. H. Chien, F. M. Hsu, P. I. Shih and C. F. Shu, *J. Mater. Chem.*, 2009, **19**, 1464.
24 S. L. Lai, Q. X. Tong, M. Y. Chan, T. W. Ng, M. F. Lo, S. T. Lee and C. S. Lee, *J. Mater. Chem.*, 2011, **21**, 1206.
25 T. M. Figueira-Duarte, P. G. D. Rosso, R. Trattnig, S. Sax, E. J. W. List and K. Mullen, *Adv. Mater.*, 2010, **22**, 990.
26 S. K. Kim, B. Yang, Y. Ma, J. H. Lee and J. W. Park, *J. Mater. Chem.*, 2008, **18**, 3376.
27 S. K. Kim, B. Yang, Y. I. Park, Y. Ma, J. Y. Lee, H. J. Kim and J. Park, *Org. Electron.*, 2009, **10**, 822.
28 S. K. Kim, Y. I. Park, I. N. Kang, J. H. Lee and J. W. Park, *J. Mater. Chem.*, 2007, **17**, 4670.
29 Y. Park, S. Kim, J. H. Lee, D. H. Jung, C. C. Wu and J. Park, *Org. Electron.*, 2010, **11**, 864.
30 B. Kim, Y. Park, J. Lee, D. Yokoyama, J. H. Lee, J. Kido and J. Park, *J. Mater. Chem. C.*, 2013, **1**, 432.
31 W. Y. Lai, R. Xia, Q. Y. He, P. A. Levermore, W. Huang and D. D. C. Bradley, *Adv. Mater.*, 2009, **21**, 355.
32 Y. Park, B. Kim, C. Lee, A. Hyun, S. Jang, J. H. Lee, Y. S. Gal, T. H. Kim, K. S. Kim and J. Park, *J. Phys. Chem. C*, 2011, **115**, 4843.
33 M. J. Frisch, G. W. Trucks, H. B. Schlegel, G. E. Scuseria, M. A. Robb, J. R. Cheeseman, G. Scalmani, V. Barone, B. Mennucci, G. A. Petersson, H. Nakatsuji, M. Caricato, X. Li, H. P. Hratchian, A. F. Izmaylov, J. Bloino, G. Zheng, J. L. Sonnenberg, M. Hada, M. Ehara, K. Toyota, R. Fukuda, J. Hasegawa, M. Ishida, T. Nakajima, Y. Honda, O. Kitao, H. Nakai, T. Vreven, J. A. Montgomery, Jr, J. E. Peralta, F. Ogliaro, M. Bearpark, J. J. Heyd, E. Brothers, K. N. Kudin, V. N. Staroverov, R. Kobayashi, J. Normand, K. Raghavachari, A. Rendell, J. C. Burant, S. S. Iyengar, J. Tomasi, M. Cossi, N. Rega, J. M. Millam, M. Klene, J. E. Knox, J. B. Cross, V. Bakken, C. Adamo, J. Jaramillo, R. Gomperts, R. E. Stratmann, O. Yazyev, A. J. Austin, R. Cammi, C. Pomelli, J. W. Ochterski, R. L. Martin, K. Morokuma, V. G. Zakrzewski, G. A. Voth, P. Salvador, J. J. Dannenberg, S. Dapprich, A. D. Daniels, Ö. Farkas, J. B. Foresman, J. V. Ortiz, J. Cioslowski and D. J. Fox, *Gaussian 09, Revision D.1*, Gaussian, Inc., Wallingford CT, 2009.